Multilevel thresholding and fractal analysis based approach for classification of brain MRI images into tumour and non-tumour

Basavaraj S. Anami

KLE Institute of Technology,
Hubli, Karnataka, India
Email: anami_basu@hotmail.com

Prakash H. Unki*

BLDEA's Dr. P.G.H. College of Engineering and Technology,
Bijapur, Karnataka, India
Email: p_unki@rediffmail.com
*Corresponding author

Abstract: In this paper, a method is proposed for classification of brain magnetic resonance imaging (MRI) images as tumour and non-tumour. A multilevel thresholding is used for segmentation. Thresholding is applied to convert MRI images to binary images. Fractal texture analysis is carried out for texture feature extraction. Mean and area features are extracted from binary images. We have computed fractal dimension (FD) using box counting method. The fractal measurements describe the boundary complexity of objects and structures beings segmented. Three features extracted, namely, mean, area and FD are used for classification. The images are classified as tumour or non-tumour using artificial neural network (ANN). The experiments are carried out on coronal, sagittal and axial views of brain MRI images. We have used the different number of thresholds (t) in the range [0–10]. We have found that the required value of t is three. Eight different parameters viz. specificity, sensitivity, accuracy, false positive rate (FPR), positive predictive value (PPV), negative predictive value (NPV), false discovery rate (FDR), F-SCORE for optimum number of thresholds are evaluated. We have obtained 100% classification accuracy for all the views of brain MRI images.

Keywords: brain MRI image; multilevel thresholding; fractal analysis; artificial neural network; ANN; tumour; classification; medical engineering.

Reference to this paper should be made as follows: Anami, B.S. and Unki, P.H. (2016) 'Multilevel thresholding and fractal analysis based approach for classification of brain MRI images into tumour and non-tumour', *Int. J. Medical Engineering and Informatics*, Vol. 8, No. 1, pp.1–13.

Biographical notes: Basavaraj S. Anami received his PhD from the University of Mysore, and MTech from Indian Institute of Technology, Chennai, both in Computer Science, in 2003 and 1986, respectively. From 1983 to 2008, he was with the Basaveshwar Engineering College, Bagalkot, India, where he worked on several research projects in image processing. Currently, he is with KLE Institute of Technology, Hubli, India, as the Principal. He visited Saginaw Valley State University, USA, as a Visiting Professor, during Fall 2006. He has authored two books and published over 100 refereed papers. He is a Fellow of

Institution of Engineers, India. He is a life member of Indian Society of Technical Education and Computer Society of India. He is a senior member of IEEE also.

Prakash H. Unki completed his BE in Electronics and Communication from Karnataka University, Dharwad, and an MTech in Computer Science and Engineering from Visvesvaraya Technological University (VTU), Belgaum, Karnataka, India, in 1996 and 2006, respectively. Currently, he is pursuing his PhD in Computer Science and Engineering from the VTU, Belgaum. Initially, he was with COE, Ambajogai, Maharashtra. Currently, he is working in BLDEA's Dr. PGH College of Engineering and Technology, Bijapur, Karnataka, as an Associate Professor in the Department of Computer Science and Engineering. He has published five papers in national and international conferences and four papers in international journals.

1 Introduction

Magnetic resonance imaging (MRI) is used to obtain images of any part of the body. The radiologists use MRI images for the visualisation of the internal structure of the body parts for diagnosis of diseases. MRI provides information about anatomy of soft tissues for diagnosis of the brain diseases such as tumour, multiple sclerosis, dementia, etc. Brain tumours are composed of cells that exhibit unrestrained growth in the brain. Brain tumor diagnosis is a very crucial task for doctors as brain tumour effects are not same for each person. The tumours even change during the treatment sessions. Brain tumours have variety of shapes and sizes. These appear at any location in the brains. Brain tumours are visible in any plane (view) in the image. In brain anatomy, there are three basic reference planes, namely, axial, sagittal and coronal. A sagittal plane of the human body is an imaginary plane that travels from the top to the bottom of the body, dividing it into left and right portions. The coronal plane divides the body into back and front portions. An axial (transverse) plane divides the body into top and bottom portions. The sample images of tumour and non-tumour images in the axial, sagittal and coronal views are as shown in Figures 1, 2 and 3 respectively.

Figure 1 Coronal views of brain MRI images, (a) tumour (b) non-tumour

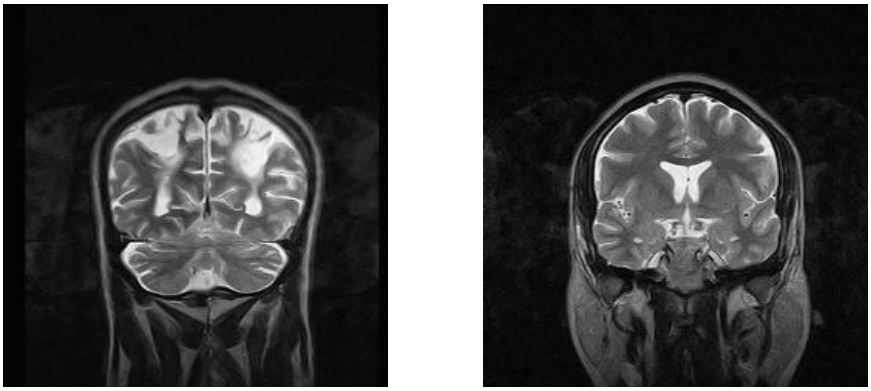

(a) (b)

Figure 2 Sagittal views of brain MRI images, (a) tumour (b) non-tumour

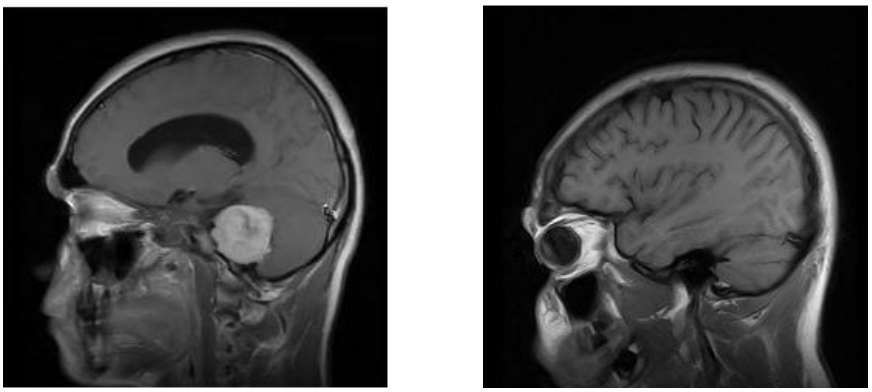

(a) (b)

Figure 3 Axial views of brain MRI images, (a) tumour (b) non-tumour

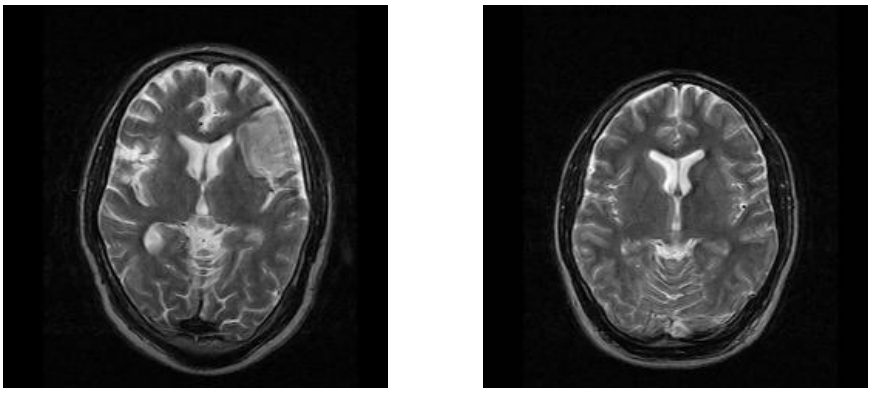

(a) (b)

As a first step, classification of brain MRI images as normal and abnormal becomes necessary. Doctors study these brain MRI images for diagnosis. Owing to human inherent limitations, it is always advisable to take leverage of computer technology in assisting the doctors for diagnosis of diseases of human brain from images. In this connection, we have carried out a literature survey. Following is the gist of papers cited in the literature related to the present work. Islam et al. (2013) have proposed a multifractal feature based brain tumour segmentation for characterising tumour texture in brain magnetic resonance (MR) images. Lopes and Betrouni (2009) have presented an overview of fractal and multifractal analysis algorithms. Fortin et al. (1992) have considered analysis of cardiac MR images and X-rays of bone using fractal dimension (FD). Anami et al. (2012) have proposed a method to classify brain MRI images as normal or abnormal. The proposed technique consists of four stages, viz. wavelet feature extraction, feature reduction using PCA, feature selection and classification using artificial neural network (ANN). Pitiot et al. (2002) have proposed an automated method for extracting anatomical structures in MRI based on texture classification. Karras and Mertzios (2003) have investigated a feature extraction approach to MRI edge detection based on identifying the critical image

edges by formulating the problem as a two-stage unsupervised classification task. Anami and Unki (2014) have proposed a reduced texture-based features' approach for classification of different views of brain MRI images viz. coronal, sagittal and axial. Sivaramakrishnan and Karnan (2013) have proposed a method for segmentation of tumours using k-nearest neighbours (k-NN) and fuzzy c-means (FCM).

From the literature survey, it is clear that various methods for analysis, segmentation and classification of brain MRI are proposed in the literature. The work on classification of brain MRI images into tumour and non-tumour is not cited much. Hence, we have developed a methodology for classification of brain MRI images. In the proposed method, multilevel thresholding, fractal analysis and ANN are used to classify brain MRI images as tumour and non-tumour images for all three planes, namely, coronal, sagittal and axial. We have demonstrated an effectiveness of the developed methodology using a set of real brain MRI images.

This paper is organised into four sections. Section 2 gives the proposed methodology. Section 3 contains results and discussion. The conclusion and future work are presented in Section 4.

2 Proposed methodology

The proposed methodology for classification of brain MRI images into tumour and non-tumour comprises of five main stages, as depicted in Figure 4. The details of each stage are as follows.

Figure 4 Stages in the proposed methodology

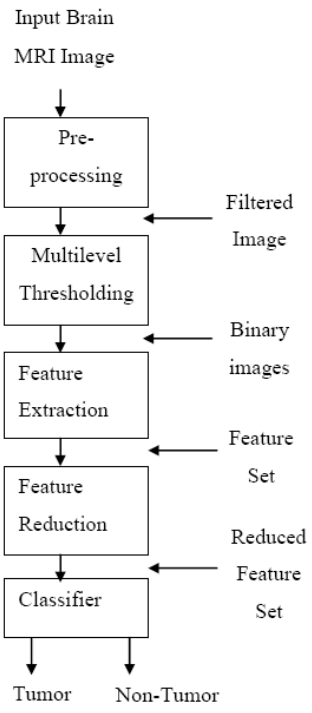

2.1 Brain MRI images and pre-processing

We have used the coronal, sagittal and axial views of brain MRI images. Each image is of size 512 * 512. The number of images in each view is 72 (36 tumour and 36 non-tumour). These images are obtained from local hospital. The MRI machine used is GE Sigma Excite of 1.5Tesla. We have considered the fluid attenuated inversion recovery (FLAIR) images. The images have 3.1 mm slice thickness (MPRAGE sequence, TR 11.4 ms, TE 4.4 ms, 128 slices). We have considered the different types of tumours such as Sarcoma, Glioma, Meningioma, MetastaticAdenocarcinoma, Glioblastoma, etc. We have considered the tumours of different size and occurring in different locations.

The research is approved by the ethical committee. The patients have given the formal consent for the research in writing and hospital provided all the resources for the research purpose. We have applied the adaptive wiener filter to reduce the presence of any degradation in the image as a pre-processing step. These images are subjected to the thresholding phase to generate binary images which is discussed in the next section.

2.2 Multilevel thresholding

The input greyscale image I is a two-dimensional function I(x, y), where I(x, y) ε {1, 2 …, R} where R is the greyscale range. The greyscale value or intensity of the pixel at position (x, y) is represented by I(x, y). By the application of successive thresholding operations, the input image is decomposed into set of binary images.

The algorithm returns a set of binary images for a given input greyscale image I(x, y). The first step of the algorithm is to find a set V of threshold values. In this work, to find the set of thresholds, we used the input image grey level distribution information by utilising the multi-level Otsu algorithm (Liao et al., 2001). The multi-level Otsu algorithm finds the threshold that minimises the input image intra-class variance. The Otsu algorithm is applied to each image region recursively until the desired number of thresholds t is obtained. We found that optimum value is 3 for the number of thresholds t. The steps involved in finding the optimum value for t are discussed in Section 2.5.

Then, we decomposed the input greyscale image into a set of binary images. This is achieved by selecting pairs of thresholds from set V of threshold values and applying two-threshold segmentation as follows.

$$\begin{aligned} B(x, y) &= 1 \text{ if } (L < I(x, y) \leq U) \\ &= 0 \text{ otherwise} \qquad \cdots\cdots \end{aligned} \tag{1}$$

where L and R denote, lower and upper threshold values respectively. B(x, y) is the binary image.

By using two threshold segmentation to the input image the set of binary images is obtained using all pairs of contiguous thresholds from V U {R} and all pairs of thresholds {t, M}, t ε V, where M corresponds to the maximum possible grey level in I(x, y). Therefore, the number of binary images generated is 2 * t, where t is the number of thresholds. The reason for using pairs of thresholds to find the set of binary images is to segment objects that would not be segmented by regular threshold segmentation.

We have started with the number of threshold t = 0 which corresponds to no thresholding and converted this image to a binary image. We have incremented the t by 1 till 10. Thresholding generates binary images at each threshold. The number of binary

images obtained at each t is given in Table 1. The feature extraction process is carried out on the binary images thus obtained. The sample binary image obtained for t = 1 is shown in Figure 5.

Table 1 Effect of number of threshold (t) on the number of binary images

Sl. no.	*t*	*No. of binary images*
1	0	1
2	1	2
3	2	4
4	3	6
5	4	8
6	5	10

Figure 5 Sample views of binary images, (a) coronal (b) sagittal (c) axial

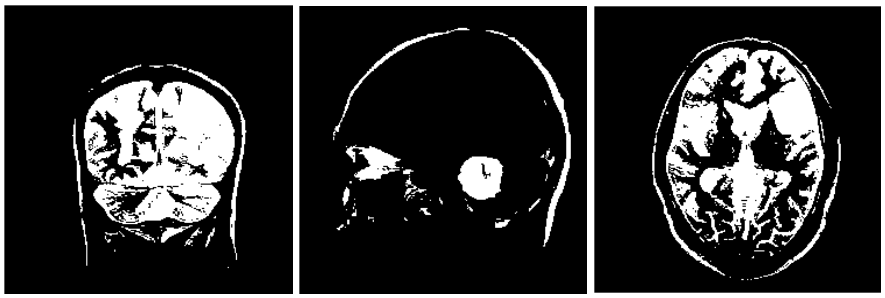

(a) (b) (c)

2.3 Feature extraction

Texture plays an important role in image analysis. It is used in various domain-specific applications such as in remote sensing, quality control and medical imaging. Additionally, texture information can be employed in image segmentation, by classifying image pixels with basis on surrounding texture information. Various texture features are used in literature for image processing applications. These include filter banks, (Manjunath and Ma, 1996), grey level co-occurrence matrices (GLCMs) (Haralick et al., 1973), etc. In these cases, we have to consider multiple orientations and scales. In applications, where large number of images is involved, the computation cost is very high.

In the image analysis, FD measurements have been used to estimate and quantify the complexity of the shape or texture of objects (Rangayyan and Nguyen, 2007; Balan et al., 2005). It is a ratio providing a statistical index of complexity comparing how detail in a fractal pattern changes with the scale at which it is measured. It has also been characterised as a measure of the space-filling capacity of a pattern that tells how a fractal scales differently than the space it is embedded in. A FD does not have to be an integer (Falconer, 2003). Various approaches to define FD are used in fractal geometry, where the most common is the Hausdorff's dimension.

Many methods are proposed to compute the FD, each one having its own theoretic basis. These algorithms are grouped into three classes: box counting, fractional Brownian motion and perimeter-area measurement (Zook and Iftekharuddin, 2005; Iftekharuddin and Parra, 2003; Novianto et al., 2003; Bisoi and Mishra, 2001; Liu et al., 2003). We have selected box counting because of its simplicity. Box counting is a method of gathering data for analysing complex patterns by breaking a dataset, object, image, etc., into smaller and smaller pieces, typically box-shaped, and analysing the pieces at each smaller scale. Computer-based box counting algorithms have been applied to patterns in one, two, and three-dimensional spaces. We have extracted the FD of an object represented by the binary image B(x, y).

We have extracted the three features from each binary image, namely, the mean grey level, area and FD. Table 2 gives the threshold value and number of features. The mean grey level is the average intensity of the binary image. The area feature is the total non-zero pixel count in the binary image. The mean grey level and area are useful additional information and they require less computation time. Algorithm 1 specifies the steps involved in the feature extraction.

Algorithm 1 Feature extraction

Input: Brain MRI image in binary form	
Output: Features set {Area, Mean, FD}	
begin	
Step 1	Compute the area and mean grey level.
Step 2	Extract the border.
Step 3	Find the fractal dimension (FD) using box counting method.
Step 4	Create a Features set {Area, Mean, FD}
end	

Table 2 Effect of threshold on the number of features

Sl. no.	*Threshold (t)*	*No. of features*
1	0	3
2	1	6
3	2	12
4	3	18
5	4	24
6	5	30

2.4 Classifier parameters

A backpropagation neural network (BPNN) is used as classifier because of its wide image processing applications in the medical field. The experiments are conducted on all three views, namely, coronal, sagittal and axial. A total of 72 (36 tumour and 36 non-tumour) images in each view are used. We have used the two output nodes and one hidden node. The number of input nodes has been changed depending on the number of input features. The termination error (TE) is set to 0.01. The learning constant η is set to 0.1. We have divided the input images into training (25%), validation (25%) and testing

(50%) randomly. The classification accuracy is defined as the correctly classified image samples divided by the total number of images. The details of calculating accuracy are specified in Section 3.

2.5 Fixing the threshold value

The number of features increases with increase in number of thresholds t. Hence, we have proposed a feedback based on accuracy method to fix the number of thresholds t to reduce the number of features. We have used the different t in the range [0–10] and we found an optimum value of three that has given 100% accuracy. We have carried out the experiment of fixing t beyond 3. Since the accuracy remained unchanged after t = 3, we have concluded that t = 3 is an optimum value. Algorithm 2 explains the steps involved in fixing the optimum number of thresholds $t_{optimum}$.

Algorithm 2 Fixing the threshold

Input: Image feature Values
Output: Optimum threshold (t) value
begin
Set t = 0;
Compute the accuracy;
While(accuracy ≤ saturation)
{
    set t = t + 1;
    Compute the accuracy;
}
$t_{optimum}$ = t;
end.

2.6 Feature reduction

The calculation complexity increases with increase in the number of threshold values because of more features. In order to reduce the number of features, we have used the average of FD, mean and area for $t_{optimum}$ and tested the methodology.

Let FD_i, $Mean_i$ and $Area_i$ denote the FD, mean pixel value and area respectively of the binary image i. Let t_n be the number of thresholds and N be the number of binary images for t_n. Let FD_{avg}, $Mean_{avg}$ and $Area_{avg}$ denote the average FD, average mean pixel value and average area respectively of the binary image B(x, y). Table 3 gives mean feature values for the $t_{optimum}$ which is 3.

Table 3 Mean feature values for optimum threshold value t = 3

Features	*Coronal*	*Sagittal*	*Axial*
FD_{avg}	1.291	1.275	1.283
$Mean_{avg}$	158.160	151.435	149.432
$Area_{avg}$	765.002	701.211	723.512

We define

$$FD_{avg} = \sum_{i=1}^{N} FD_i / N \quad \ldots\ldots \quad (2)$$

$$Mean_{avg} = \sum_{i=1}^{N} Mean_i / N \quad \ldots\ldots \quad (3)$$

$$Area_{avg} = \sum_{i=1}^{N} Area_i / N \quad \ldots\ldots \quad (4)$$

2.7 Overall methodology

Images of brain MRI are in coronal, sagittal and axial views. Maximum threshold value (maxT) is set to 10 arbitrarily and initial number of thresholds (t) is set to 0. The overall methodology for classification of images as tumour and non-tumour using multilevel thresholding, fractal analysis and classifier is given in Algorithm 3.

Algorithm 3 Classification of brain MRI images

Input: Brain MRI images with tumour and non-tumour in Coronal, Sagittal and Axial Views

Output: Classification of images as tumour and non-tumour

begin

For all input images

{

Step 1 Accept input image.

Step 2 Apply thresholding for optimum value of t to generate binary images.

Step 3 Extract the features FD, mean grey level, and area for each binary image.

Step 4 Find the mean value of features FD_{avg}, $Mean_{avg}$ and $Area_{avg}$ across all binary images.

Step 5 Store mean feature values in a database.

}

Step 6 Divide the input images into training (25%), validation (25%) and testing (50%) randomly.

Step 7 Train and Test ANN classifier with features stored in database.

Step 8 Calculate parameters accuracy, specificity, sensitivity, False Positive Rate (FPR), Positive Predictive Value (PPV), Negative Predictive Value (NPV), False Discovery Rate (FDR) and F-SCORE.

end

3 Results and discussions

The methodology is coded using MATLAB Version 7.11(Release R2010b) and implemented on laptop with Intel(R) Core™ i3-2350M CPU @ 2.3GHz and 4GB RAM running Microsoft Windows 7.

We have used a three layer ANN to obtain the classification of images under two categories, namely, tumour and non-tumour. The number of input neurons for the ANN is

based on the number of input features. The number of neurons in the output layer is 2, which corresponds to two categories of images. The number of neurons used in hidden nodes is 5, which is selected based on trial and error. The training process is carried out with back-propagation, until 1,000 epochs or the maximum acceptable mean square error (MSE) is reached. The training algorithm used is scaled conjugate gradient. The performance is measured using MSE criterion. The data division is random. The input data is divided into training (25%), validation (25%) and testing (50%) randomly. The extracted features are used after normalisation to train the ANN.

We have calculated the accuracy by repeating the experiment ten times and finding the mean values. To calculate the accuracy, we have used the testing group.

Let

TP true positive, tumour image identified as tumour

TN true negative, non-tumour image identified as non-tumour

FP false positive, non-tumour image identified as tumour

FN false negative, tumour image identified as non-tumour.

The accuracy is obtained using expression (5).

$$\text{Accuracy} = \frac{(\text{TP}+\text{TN})}{(\text{TP}+\text{FP}+\text{TN}+\text{FN})} * 100 \quad \ldots\ldots \quad (5)$$

We have conducted experiments to test the classification accuracies for non-tumour (normal) and tumour images in coronal, sagittal and axial views and the results are plotted as shown in Figures 6, 7 and 8 respectively.

Figure 6 Classification accuracy of non-tumour and tumour images in coronal view (see online version for colours)

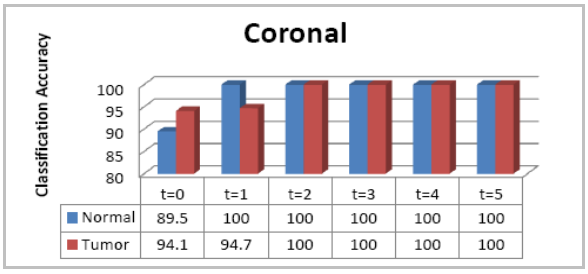

Figure 7 Classification accuracy of non-tumour and tumour images in sagittal view (see online version for colours)

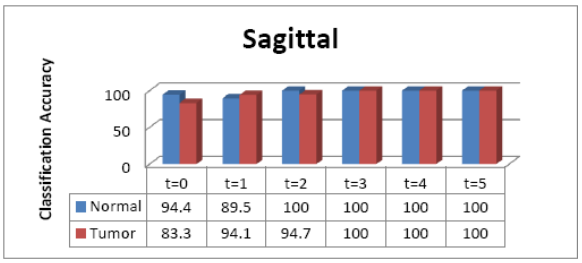

Figure 8 Classification accuracy of non-tumour and tumour images in axial view (see online version for colours)

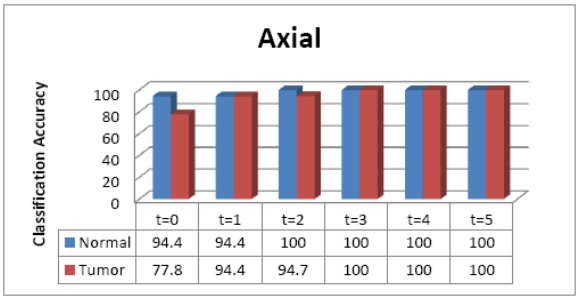

We have changed the number of thresholds (t) from 0 until the classification accuracy reaches the saturation (100%). From the graphs, it is observed that from t = 3 onwards the accuracy has reached saturation. Hence, we have fixed the optimum threshold $t_{optimum}$ as 3. However, for coronal images the saturation has reached at t = 2. We have drawn the confusion matrix for all views as shown in Table 4. We have observed that the accuracy has reached saturation for t = 3 and it is found to be 100% for all the three views.

Table 4 Confusion matrix for different views

t	*0*		*1*		*2*		*3*		*4*		*5*	
						Coronal						
	N	*T*	*N*	*T*	*N*	*T*	*N*	*T*	*N*	*T*	*N*	*T*
N	17	2	17	0	18	0	18	0	18	0	18	0
T	1	16	1	18	0	18	0	18	0	18	0	18
						Sagittal						
N	17	3	17	2	17	0	18	0	18	0	18	0
T	1	15	1	16	1	18	0	18	0	18	0	18
						Axial						
N	17	4	17	1	17	0	18	0	18	0	18	0
T	1	14	1	17	1	18	0	18	0	18	0	18

Notes: t – threshold, N – normal, T – tumour.

The eight different parameters viz. specificity, sensitivity, accuracy, false positive rate (FPR), positive predictive value (PPV), negative predictive value (NPV), false discovery rate (FDR) and F-SCORE are calculated using the confusion matrix. The different parameters calculated for t = 3 for all three views are shown in Figure 9. The details of these parameters are found in http://en.wikipedia.org/wiki/Sensitivity_and_specificity.

From graphs given in Figure 9, it is clear that the proposed method gives 100% result for the parameters specificity, sensitivity, accuracy PPV, NPV and F-SCORE. The parameters FPR and FDR are 0%. Pauline (2012) has used brain tumour classification using wavelet and texture-based neural network but the author has considered the images only in the axial view and used features extracted using GLCM which are computationally expensive. Hence, the proposed method gives accuracy of 100% for all views and using only few features.

Figure 9 Different parameters for number of thresholds t = 3 for all views (see online version for colours)

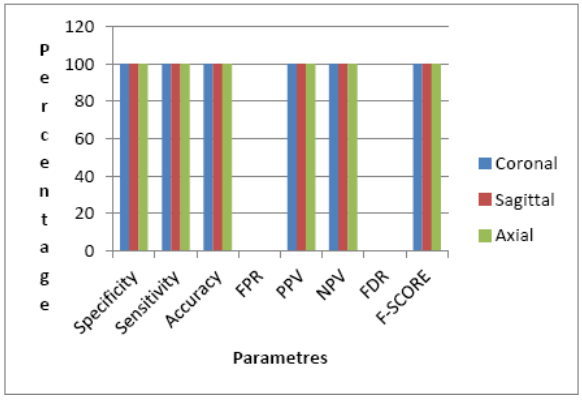

Notes: FPR – false positive rate, PPV – positive predictive value, NPV – negative predictive value, FDR – false discovery rate.

4 Conclusions

Classification of tumour and non-tumour brain MRI images is carried out, wherein segmentation using multilevel thresholding, fractal texture analysis and ANN-based classifier is deployed. Three features, namely, mean, area and FD are used. The experiments are carried out with different number thresholds (t) values in the range [1–10]. We have found that t = 3 is the optimum value. The results are verified using real brain MRI images in coronal, sagittal and axial views. Eight different parameters are used for testing the methodology. The classification accuracy of 100% is observed for all views of brain MRI images.

References

Anami, B.S. and Unki, P.H. (2014) 'Reduced texture based features' approach for identification of different views of brain MRI images', *International Journal of Tomography & Simulation*, Vol. 25, No. 1, pp.86–100.

Anami, B.S., Unki, P.H. and Anvekar, B.T. (2012) 'A wavelet based reduced feature set for classification of brain MRI images into normal and abnormal', *International Journal of Tomography & Simulation*, Vol. 21, No. 3, pp.18–32.

Balan, A.G.R., Traina, A.J.M., Traina, C. Jr. and Marques, P.M.A. (2005) 'Fractal analysis of image textures for indexing and retrieval by content', *18th IEEE Symposium on Computer-Based Medical Systems (CBMS'05)*, pp.581–586.

Bisoi, A.K. and Mishra, J. (2001) 'On calculation of fractal dimension of images', *Pattern Recognition Letters*, Vol. 22, Nos. 6–7, pp.631–637.

Falconer, K. (2003) *Fractal Geometry*, p.308, Wiley, New York.

Fortin, C., Kumaresan, R., Ohley, W. and Hoefer, S. (1992) 'Fractal dimension in the analysis of medical images', *IEEE Transactions on Engineering in Medicine and Biology*, Vol. 11, No. 2, pp.65–71.

Haralick, R.M., Shanmugam, K. and Dinstein, I.H. (1973) 'Textural features for image classification', *IEEE Transactions on Systems, Man and Cybernetics*, Vol. 3, No. 6, pp.610–621.

Iftekharuddin, K. and Parra, C. (2003) 'Multiresolution-fractal feature extraction and tumor detection: analytical model and implementation', *Optical Science and Technology, SPIE's 48th Annual Meeting International Society for Optics and Photonics*, pp.801–812.

Islam, A., Reza, S. and Iftekharuddin, K. (2013) 'Multi-fractal texture estimation for detection and segmentation of brain tumors', *IEEE Transactions on Biomedical Engineering*, Vol. 60, No. 11, pp.3204–3215.

Karras, D.A. and Mertzios, B.G. (2003) 'On edge detection in MRI using the wavelet transform and unsupervised neural networks', *Video/Image Processing and Multimedia Communications, 2003: 4th EURASIP Conference Focused on*, Vol. 2, pp.461–466.

Liao, P., Chen, T. and Chung, P. (2001) 'A fast algorithm for multilevel thresholding', *Journal of Information Science and Engineering*, Vol. 17, No. 5, pp.713–727.

Liu, J.Z., Zhang, L.D. and Yue, G.H. (2003) 'Fractal dimension in human cerebellum measured by magnetic resonance imaging', *Biophysical Journal*, Vol. 85, No. 6, pp.4041–4046.

Lopes, R. and Betrouni, N. (2009) 'Fractal and multifractal analysis: a review', *Medical Image Analysis*, Vol. 13, No. 4, pp.634–649.

Manjunath, B.S. and Ma, W.Y. (1996) 'Texture features for browsing and retrieval of image data', *IEEE Transactions on Pattern Analysis and Machine Intelligence*, Vol. 18, No. 8, pp.837–842.

Novianto, S., Suzuki, Y. and Maeda, J. (2003) 'Near optimum estimation of local fractal dimension for image segmentation', *Pattern Recognition Letters*, Vol. 24, Nos. 1–3, pp.365–374.

Pauline, J. (2012) 'Brain tumor classification using wavelet and texture based neural network', *International Journal of Scientific & Engineering Research*, Vol. 3, No. 10, pp.1–7.

Pitiot, A., Toga, A., Ayache, W.N. and Thompson, P. (2002) 'Texture based MRI segmentation with a two-stage hybrid neural classifier', *Neural Networks, 2002, IJCNN'02: Proceedings of the 2002 International Joint Conference on*, Vol. 3, pp.2053–2058.

Rangayyan, R.M. and Nguyen, T.M. (2007) 'Fractal analysis of contours of breast masses in mammograms', *Journal of Digital Imaging*, Vol. 20, No. 3, pp.223–237.

Sivaramakrishnan, A. and Karnan, M. (2013) 'A novel based approach for extraction of brain tumor in MRI images using soft computing techniques', *International Journal of Advanced Research in Computer and Communication Engineering*, Vol. 2, No. 4, pp.1845–1848.

Zook, J. and Iftekharuddin, K. (2005) 'Statistical analysis of fractal-based brain tumor detection algorithms', *Magnetic Resonance Imaging*, Vol. 23, No. 5, pp.671–678.

Websites

http://en.wikipedia.org/wiki/Sensitivity_and_specificity.